Applications of Parallel Computing Technologies for Modeling the Flow Separation Process behind the Backward Facing Step Channel with the Buoyancy Forces

A. Issakhov(✉), A. Abylkassymova, and M. Sakypbekova

Al-Farabi Kazakh National University, Almaty, Kazakhstan
alibek.issakhov@gmail.com

Abstract. Taking into account the high rate of construction in the modern big cities, it is very important to save the natural aerodynamics between the buildings. It is necessary to explore the ventilation of space between architectural structures, making a preliminary prediction before construction starting. The most optimal way of evaluating is to build a mathematical model of air flow. This paper presents numerical solutions of the wind flow around the architectural obstacles with the vertical buoyancy forces. An incompressible Navier-Stokes equation is used to describe this process. This system is approximated by the control volume method and solved numerically by the projection method. The Poisson equation that is satisfying the discrete continuity equation solved by the Jacobi iterative method at each time step. For check correctness of mathematical model and numerical algorithm is solved test problem. The numerical solutions of the backward-facing step flow with the vertical buoyancy forces, which was compared with the numerical results of other authors. This numerical algorithm is completely parallelized using various geometric domain decompositions (1D, 2D and 3D). Preliminary theoretical analysis of the various decomposition methods effectiveness of the computational domain and real computational experiments for this problem were made and the best domain decomposition method was determined. In the future, a proven mathematical model and parallelized numerical algorithm with the best domain decomposition method can be applied for various complex flows with the vertical buoyancy forces.

Keywords: Domain decomposition method · Flow around the architectural obstacles · Backward-facing step flow · Projection method · Vertical buoyancy forces · Mixed convection

1 Introduction

The increased pace of construction in modern large cities and, in particular, Almaty, leads to a tightening of architectural structures. Due to the increase in

Y. Shokin and Z. Shaimardanov (Eds.): CITech 2018, CCIS 998, pp. 97–113, 2019.
https://doi.org/10.1007/978-3-030-12203-4_10

the population of cities and to save space, mostly high-rise multi-storey buildings are being built. As a consequence, this entails such consequences as a violation of the natural aerodynamics of the city, which in turn leads to increased gas contamination of the city, the accumulation of heavy metals in the lower atmosphere, and to the violation of the local climate. The building codes and norms currently used in the construction and design of buildings do not contain aerodynamic criteria and coefficients indicating the optimal distance between buildings of different heights. When determining these standards, various natural and climatic features are taken into account, such as wind loads, insolation, etc. Fire safety requirements are also taken into account. However, the above-mentioned documents do not take into account the factor of natural aerodynamics of space between neighboring buildings. The distance between buildings and structures is considered to be the distance between the outer walls or other structures. As a result, when designing, the distances between building objects are laid, which can not provide free movement of the wind vortex, which leads to a disturbance of the natural air flow. In this thesis, a model of aerodynamics between two high-rise buildings is considered. This mathematical model allows you to accurately calculate the optimal distance between the two buildings, which will take into account the climatic features and will preserve the natural purge. In many technical flows of practical interest, like flow divisions, with the sudden expansion of geometry or with subsequent re-joining, are a common occurrence. The existence of a flow separation and recirculation area has a significant effect on the performance of heat transfer devices, for example, cooling equipment in electrical engineering, cooling channels of turbine blades, combustion chambers and many other heat exchanger surfaces that appear in the equipment. Many papers are devoted to the motion of a fluid with separation and reconnection of flows without taking into account the buoyancy forces. The importance of this process is indicative of the number of papers where special attention was paid to building equipment [1–3] and developing experimental and theoretical methods for detailed study of flows with separation regions [4–7,28–30]. An extensive survey of isothermal flows in fluid flows is given in papers [10–12]. Heat transfer in the flows has been investigated by many authors, like Aung [13,14], Aung et al. [15], Aung and Worku [16], Sparrow et al. [17,18] and Sparrow and Chuck [19]. However, published papers on this topic do not take into account the strength of buoyancy force on the flow stream or the characteristics of heat transfer. These effects become significant in the laminar flow regime, where the velocity is relatively low, and when the temperature difference is relatively high. Ngo and Byon [26] studied the location effect of the heater and the size of the heater in a two-dimensional square cavity using the finite element method. Oztop and Abu-Nada [27] numerically investigated natural convection in rectangular shells, partially heated from the side wall by the finite volume method. In this paper considered the influence of buoyancy forces on the flow and heat transfer characteristics in individual flows. Numerical solutions for a laminar mixed convective airflow ($\mathrm{Pr} = 0.7$) in a vertical two-dimensional channel with a backward-facing step to maintain the buoyancy effect are shown in Fig. 1. Numerical results of interest,

such as velocity and temperature distributions, re-binding lengths and friction coefficients are presented for the purpose of illustrating the effect of buoyancy forces on these parameters.

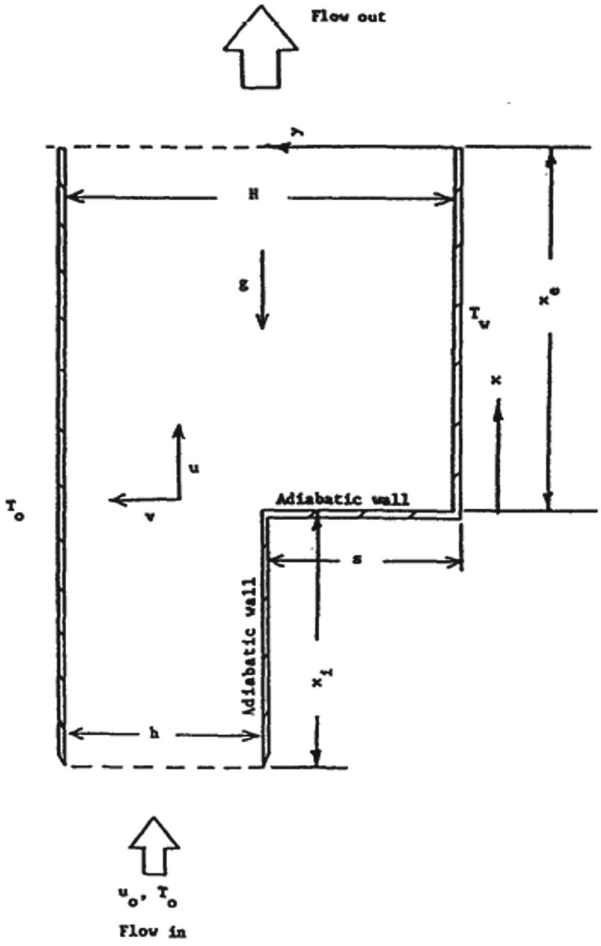

Fig. 1. Schematic representation of the backward-facing step flows.

2 Mathematical Formulation of the Problem

Consider a two-dimensional laminar convective flow in a vertical channel with a sudden expansion behind the inverse step of height s, as shown in Fig. 1. The straight wall of the channel is maintained at a uniform temperature equal to the temperature of the inlet air T_0. The stepped wall below the stage is heated to a

uniform temperature, which can be adjusted to any desired value T_w. The upper part of the stepped wall and the reverse side is installed as an adiabatic surface. The inlet length of the channel x_i and the outlet lower length x_e of the channel are appropriate dimensions. These lengths are assumed to be infinite, but the simulation domain is limited by the length $L_e = x_e + x_i$. The smaller section of the channel before the projection has a height, and the large section below the stage has a height $H = h + s$. Air flows up the channel with mean velocity $u_0$and uniform temperature T_0. The gravitational force g in this problem is considered to act vertically downwards.

To describe this physical problem, was used assumption about constant properties, and was used the Boussinesq approximation. This system of equations in an immense form can be written in the form:

$$\frac{\partial U}{\partial X} + \frac{\partial V}{\partial Y} = 0 \tag{1}$$

$$\frac{\partial U}{\partial t} + U\frac{\partial U}{\partial X} + V\frac{\partial U}{\partial Y} = -\frac{\partial P}{\partial X} + \frac{1}{Re}\left(\frac{\partial^2 U}{\partial X^2} + \frac{\partial^2 U}{\partial Y^2}\right) + \frac{Gr}{Re^2}\theta \tag{2}$$

$$\frac{\partial V}{\partial t} + U\frac{\partial V}{\partial X} + V\frac{\partial V}{\partial Y} = -\frac{\partial P}{\partial Y} + \frac{1}{Re}\left(\frac{\partial^2 V}{\partial X^2} + \frac{\partial^2 V}{\partial Y^2}\right) \tag{3}$$

$$\frac{\partial \theta}{\partial t} + U\frac{\partial \theta}{\partial X} + V\frac{\partial \theta}{\partial Y} = \frac{1}{\Pr\, Re}\left(\frac{\partial^2 \theta}{\partial X^2} + \frac{\partial^2 \theta}{\partial Y^2}\right) \tag{4}$$

The dimensionless parameters in the equations given above are defined by the formula:

$$U = u/u_0, \quad V = \upsilon/u_0, \quad X = x/s, \quad Y = y/s,$$

$$\theta = (T - T_0)/(T_w - T_0), \quad P = p/\rho_0 u_0^2,$$

$$\Pr = \nu/\alpha, \quad Re = u_0 s/\nu, \quad Gr = g\beta\,(T_w - T_0)\,s^3/\nu^2.$$

Where α – the temperature diffusion, ν – the kinematic viscosity, and β – the thermal expansion coefficient are estimated at the film temperature $T_f = (T_0 + T_w)/2$ (Fig. 2).

Boundary conditions:

(a) Inlet conditions: At the point $X = -X_i$ and $1 \le Y \le H/s$: $U = u_i/u_0$, $V = 0$, $\theta = 0$, $\frac{\partial p}{\partial x} = -\frac{Gr}{Re^2}\theta$.
where u_i is the local distribution of velocities at the inlet, which is assumed to have a parabolic profile and u_i/u_0 an average inlet velocity, that is, given by formula

$$u_i/u_0 = 6\left[-y^2 + (H+s)y - Hs\right]/(H-s)^2$$

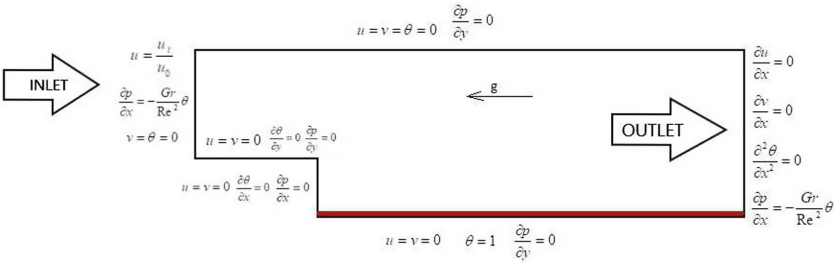

Fig. 2. Boundary conditions.

(b) Outlet conditions: At the point $X = X_e$ and $0 \le Y \le H/s$: $\partial U/\partial X = 0$, $\partial^2\theta/\partial X^2 = 0$, $\partial V/\partial X = 0$, $\frac{\partial p}{\partial x} = -\frac{Gr}{Re^2}\theta$.
(c) on the top wall: At the point $Y = H/s$ and $-X_i \le X \le X_e$: $U = 0$, $V = 0$, $\theta = 0$, $\frac{\partial p}{\partial y} = 0$.
(d) on the wall of the upper stage: At the point $Y = 1$ and $-X_i \le X < 0$: $U = 0$, $V = 0$, $\partial\theta/\partial Y = 0$, $\frac{\partial p}{\partial y} = 0$.
(e) on the wall of the lower stage: At point $X = 0$ and $0 \le Y \le 1$: $U = 0$, $V = 0$, $\partial\theta/\partial X = 0$, $\frac{\partial p}{\partial x} = 0$.
(f) on the wall below the stage: At the point $Y = 0$ and $0 \le X \le X_e$: $U = 0$, $V = 0$, $\theta = 1$, $\frac{\partial p}{\partial y} = 0$.

The last term on the right-hand side of Eq. (2) is the contribution of the buoyancy force. The length of the downstream flow from the simulation area was chosen to be 70 steps ($X_e = 70$). The upper length of the design area was chosen to be 5 steps (i.e. $X_i = 5$), and the velocity profile at the input area was set as parabolic profile, like $u_i/u_0 = 6\left[-y^2 + (H+s)y - Hs\right]/(H-s)^2$, and temperature was chosen as uniform T_0.

3 The Numerical Algorithm

For a numerical solution of this system of equations, the projection method is used [8,20–23,36]. The equations are approximated by the finite volume method [20,24,35–38]. At the first stage it is assumed that the transfer of momentum is carried out only through convection and diffusion, and an intermediate velocity field is calculated by the fourth-order Runge-Kutta method [21,22,31–34,36]. At the second stage, according to the found intermediate velocity field, there is a pressure field. The Poisson equation for the pressure field is solved by the Jacobi method. At the third stage it is assumed that the transfer is carried out only due to the pressure gradient. At the fourth stage, the equations for the temperature are calculated by the fourth-order Runge-Kutta method [21,22,31–34,36].

$$I. \qquad \int_\Omega \frac{\boldsymbol{u}^* - \boldsymbol{u}^n}{\Delta t} d\Omega = -\oint_{\partial\Omega} (\boldsymbol{u}^n \boldsymbol{u}^* - \frac{1}{Re}\nabla \boldsymbol{u}^*) n_i d\Gamma - \int_\Omega \frac{Gr}{Re^2}\theta d\Omega,$$

$$II. \quad \oint_{\partial\Omega} (\nabla p) d\Gamma = \int_{\Omega} \frac{\nabla \boldsymbol{u}^*}{\Delta t} d\Omega,$$

$$III. \quad \frac{\boldsymbol{u}^{n+1} - \boldsymbol{u}^*}{\Delta t} = -\nabla p,$$

$$IV. \quad \int_{\Omega} \frac{\theta^* - \theta^n}{\Delta t} d\Omega = -\oint_{\partial\Omega} (\boldsymbol{u}^n \theta^* - \frac{1}{Re \, \mathrm{Pr}} \nabla \theta^*) n_i d\Gamma,$$

4 Parallelization Algorithm

For numerical simulation was constructed a computational mesh by using the PointWise software. The problem was launched on the ITFS-MKM software using a high-performance computing. The equations are approximated by the finite volume method (FVM) and used collocated grid, because it makes parallisation of numerical algorithm simple and efficient to use domain decomposition method. For pressure velocity coupling is used Rhie-Chow interpolation. This coupling interpolate pressure on the faces of the cell and then use this face pressure to construct the central difference scheme for pressure, which couples the adjacent pressures and avoid the checkerboard effect. For convective flux term used first order upstream flow scheme. This numerical algorithm is completely parallelized using various geometric domain decompositions (1D, 2D and 3D). Geometric partitioning of the computational grid is chosen as the main approach of parallelization. In this case, there are three different ways of exchanging the values of the grid function on the computational nodes of a one-dimensional, two-dimensional, and three-dimensional mesh. After the domain decomposition stage, when parallel algorithms are built on separate blocks, a transition is made to the relationships between the blocks, the simulations on which will be executed in parallel on each processor. For this purpose, a numerical solution of the equation system was used for an explicit scheme, since this scheme is very efficiently parallelized. In order to use the domain decomposition method as a parallelization method, this algorithm uses the boundary nodes of each subdomain in which it is necessary to know the value of the grid function that borders on the neighboring elements of the processor. To achieve this goal, at each compute node, ghost points store values from neighboring computational nodes, and organize the transfer of these boundary values necessary to ensure homogeneity of calculations for explicit formulas [36].

Data transmission is performed using the procedures of the MPI library [25]. By doing preliminary theoretical analysis of the effectiveness of various domain decomposition methods of the computational domain for this problem, which will estimate the time of the parallel program as the time T_{calc} of the sequential program divided by the number of processors plus the transmission time $T_p = T_{calc}/p + T_{com}$. While transmissions for various domain decomposition methods can be approximately expressed through capacity [36]:

$$\begin{aligned} T_{com}^{1D} &= t_{send} 2N^2 \times 2 \\ T_{com}^{2D} &= t_{send} 2N^2 \times 4p^{1/2} \\ T_{com}^{3D} &= t_{send} 2N^2 \times 6p^{2/3} \end{aligned} \tag{5}$$

where N^3 – the number of nodes in the computational mesh, p - the number of processors (cores), t_{send} – the time of sending one element (number).

It should be noted that for different decomposition methods, the data transmission cost can be represented as $T_{com}^{1D} = t_{send} 2N^2 x k(p)$ in accordance with the formula (5), where $k(p)$ is the proportionality coefficient, which depends on the domain decomposition method and the number of processing elements used [36].

At the first stage, one common program was used, the size of the array from start to run did not change, and each element of the processor was numbered by an array of elements, starting from zero. For the test simulation is used well known problem – 3D cavity flow. Despite the fact that according to the theoretical analysis of 3D decomposition is the best option for parallelization (Fig. 3), computational experiments showed that the best results were achieved using 2D decomposition, when the number of processes varies from 25 to 144 (Fig. 3) [36].

Based on the preliminary theoretical analysis of the graphs, the following character can be noted. The simulation time without the interprocessor communications cost with different domain decomposition methods should be approximately the same for the same number of processors and be reduced by T_{calc}/p. In fact, the calculated data show that when using 2D decomposition on different computational grids, the minimal cost for simulation and the cost graphs are much higher, depending on the simulation time, on several processors taken T_{calc}/p [36].

To explain these results, it is necessary to pay attention to the assumptions made in the preliminary theoretical analysis of efficiency for this task. First, it was assumed that regardless of the distribution of data per processor element, the same amount of computational load was done, which should lead to the same time expenditure. Secondly, it was assumed that the time spent on interprocessor sending's of any degree of the same amount of data is not dependent on their memory choices. In order to understand what is really happening, the following sets of computational simulations test were carried out. For evaluation, the sequence of the first approach was considered when the program is run in a single-processor version, and thus simulates various geometric domain decomposition methods of data for the same amount of computation performed by each processor [36].

5 Numerical Results for Test Problem

Geometric parameters are indicated in Fig. 1: channel length L = 75, channel height H = 2, step height S = 1. Numerical results were obtained for the dimensionless numbers Re = 50, Pr = 0.7 and Gr = 19.1 [9].

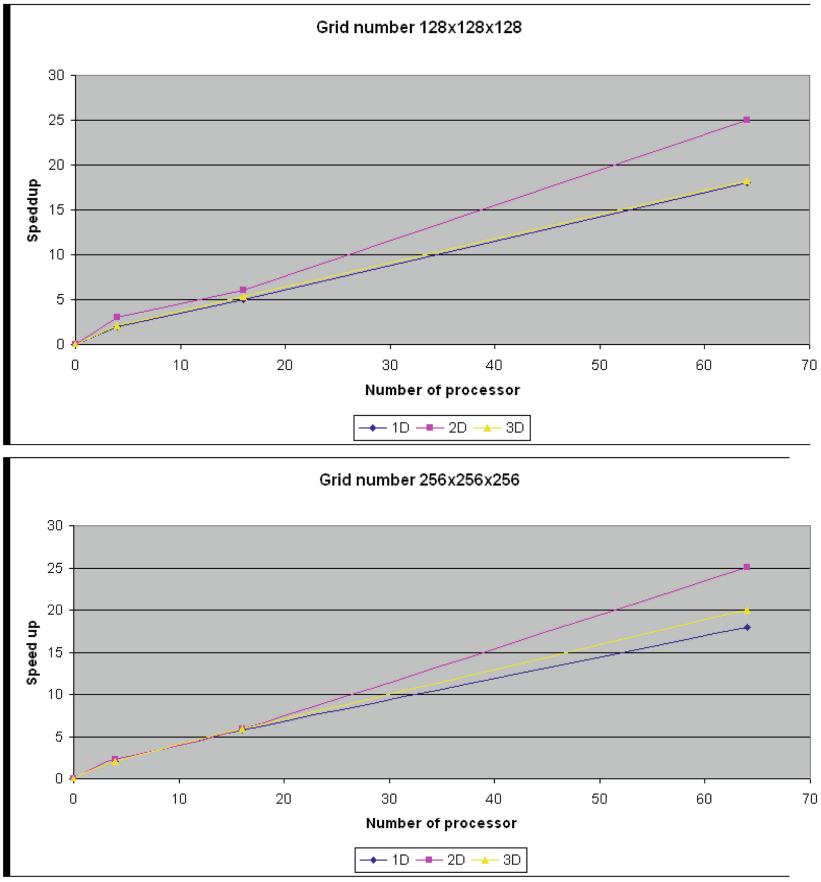

Fig. 3. Speed-up for various domain decomposition methods of the computational domain.

Figure 4 shows the comparison of the longitudinal velocity profile with the numerical data of Lin et al. [9] at the point $x/x_f = 0.5$, where $x_f = 2.91$. Figure 5 shows the comparison of temperature profiles with the numerical data of Lin et al. [9] at the point $x/x_f = 0.5$, where $x_f = 2.91$. It can be seen from the figures that the mathematical model and the numerical algorithm which is used in this paper is coincided with the numerical results obtained by Lin et al. [9]. Figure 6 shows the streamlines and the horizontal velocity contour for dimensionless numbers $\mathrm{Re} = 50$, $\mathrm{Pr} = 0.7$ and $\mathrm{Gr} = 19.1$. Figure 7 shows the vertical velocity contour for dimensionless numbers $\mathrm{Re} = 50$, $\mathrm{Pr} = 0.7$ and $\mathrm{Gr} = 19.1$. Figure 8 shows the temperature profile for dimensionless numbers $\mathrm{Re} = 50$, $\mathrm{Pr} = 0.7$ and $\mathrm{Gr} = 19.1$. For a better understanding of this process from Figs. 6, 7 and 8 can be seen

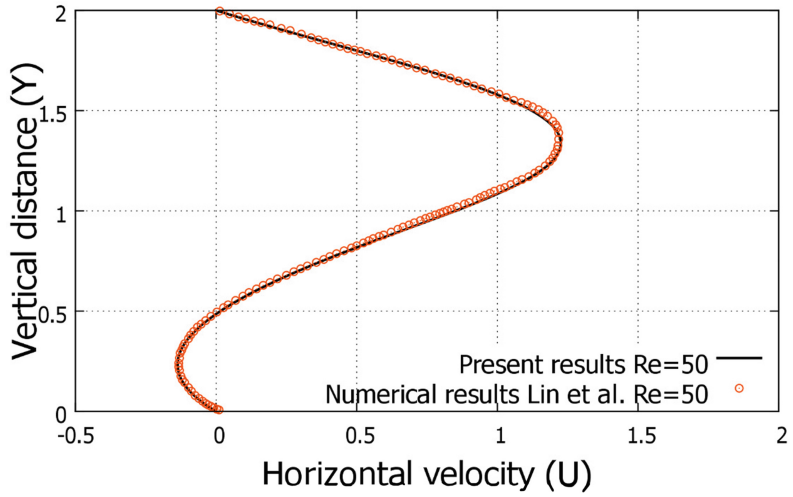

Fig. 4. Velocity profile with vertical buoyancy forces for dimensionless number $\mathrm{Re} = 50$, $\Delta T = 1\,^{\circ}\mathrm{C}$, $x/x_f = 0.5$, where $x_f = 2.91$.

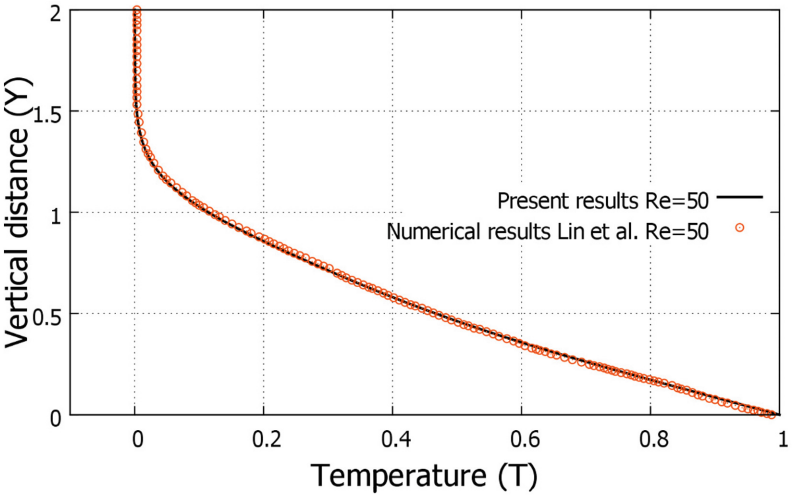

Fig. 5. Temperature profile with vertical buoyancy forces for dimensionless number $\mathrm{Re} = 50$, $\Delta T = 1\,^{\circ}\mathrm{C}$, $x/x_f = 0.5$, where $x_f = 2.91$.

the development of the backward-facing step flow with vertical buoyancy force: the initiation and process of the development of the region of flows reconnection with taking into account the buoyancy forces.

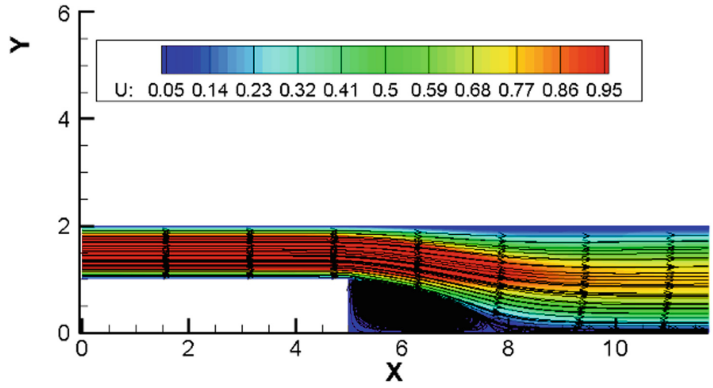

Fig. 6. The contour of the horizontal velocity component with streamlines for dimensionless numbers Re = 50, Pr = 0.7 and Gr = 19.1.

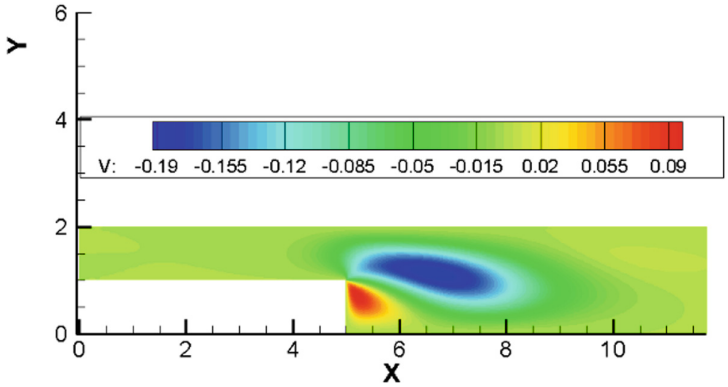

Fig. 7. The contour of the vertical velocity component for dimensionless numbers Re = 50, Pr = 0.7 and Gr = 19.1.

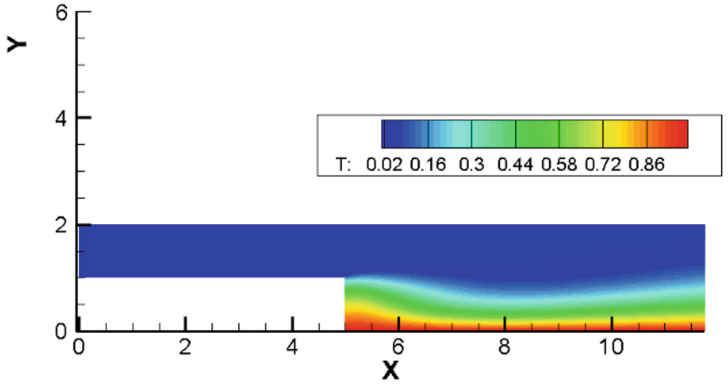

Fig. 8. Temperature contour for dimensionless numbers Re = 50, Pr = 0.7 and Gr = 19.1.

6 Numerical Results for Real Problem

For the real problem considered a man-made obstacle 9 floors (27 m) and 5 floors (15 m) buildings. The wind flow is conventionally moving from the high building side to the low one. The following models consider the calm, according to the Beaufort wind speed scale. The speed of wind is in the range from 0 to 0.2 m/s. To find the optimal distance, various parameters prescribed in the above-mentioned standards were used.

According to the fire protection requirements specified in Building norms and regulations of the Republic of Kazakhstan 3.01-01-2002, 2.12 * [18], the minimum distance between houses with a height of 4 floors or more must be at least 20 m. However, having constructed this model, a result was obtained, showing that at such a distance between the buildings, there was no wind, therefore, air circulation does not occur in this interval.

After that, the IBC (International Building Code) standard used in the USA was considered, where the distance between two buildings is calculated according to the following formula (Fig. 9) [19]:

$$\delta_{MT} = \sqrt{(\delta_{M1})^2 + (\delta_{M2})^2}$$

where δ_{MT} - required distance, δ_{M1}, δ_{M2} - height of the first and second buildings, respectively.

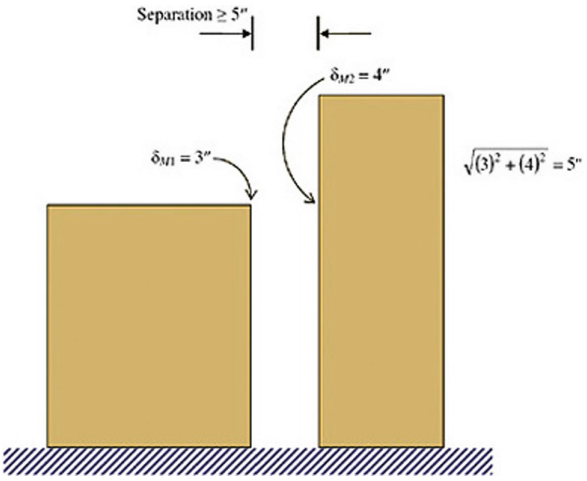

Fig. 9. The calculation of the distance between two high-rise buildings according to IBC 2009 1613.6.7

For the calculations, the area was divided into the 14 design subareas of different sizes. Each subregion is a grid block, which contains a part of a curvilinear, uneven, unstructured grid. When creating a grid, the number of points

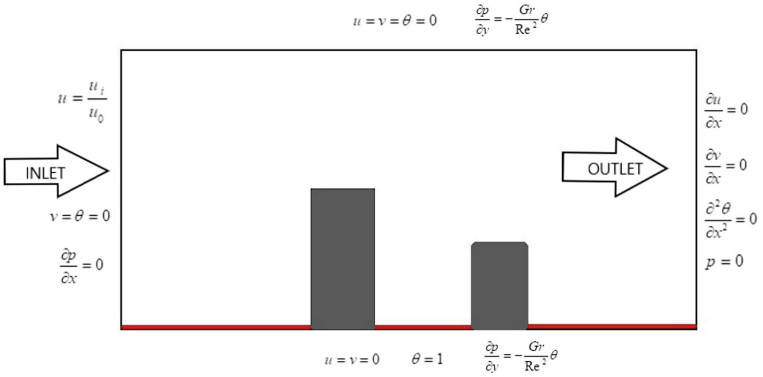

Fig. 10. Boundary conditions

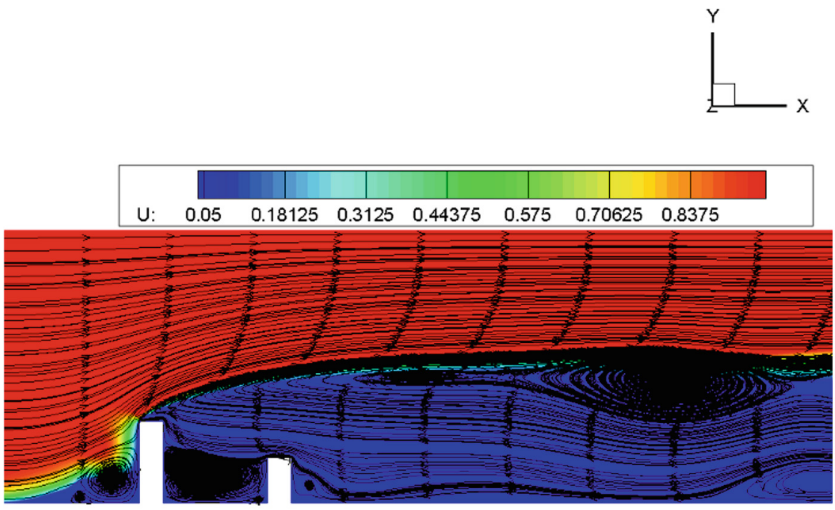

Fig. 11. Horizontal velocity-component and streamlines with buoyancy force for Pr = 0.7 and $\Delta T = 1\,^{\circ}\mathrm{C}$.

is chosen in such a way that no oscillations occur in the solution of the problem and the results are correct for large values of the Reynolds number. Thus, the constructed grid contains more than 100 000 control volumes.

In the interval between the buildings and near the streamlined surfaces of buildings, the grid is thickened, i.e. the sizes of control volumes decrease. This allows for more accurate simulations. As the grid is removed from the vortex zone and the dimensions of the control volumes increase the flow around. Therefore, in areas that are not of great interest in solving a given problem, net catch is smaller. And in the most important zones for the model, the number of nodes is greater, which allows obtaining more accurate results.

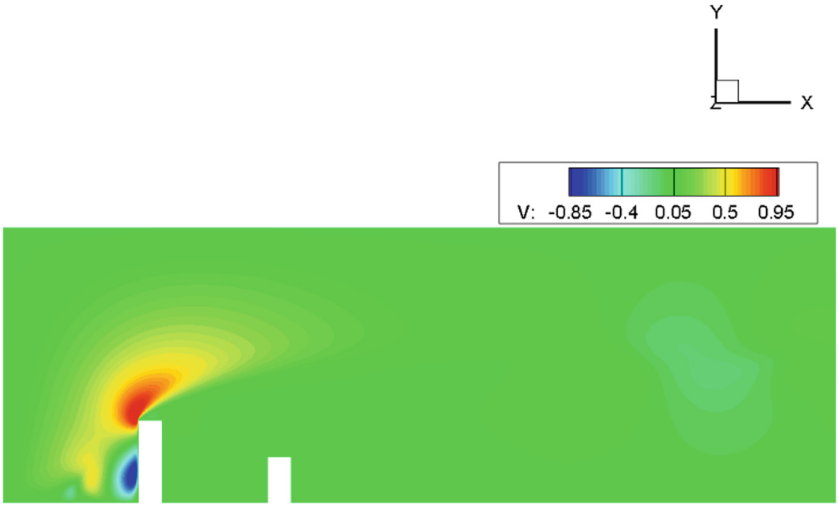

Fig. 12. Vertical velocity-component with buoyancy force for Pr = 0.7 and $\Delta T = 1\,^{\circ}\mathrm{C}$.

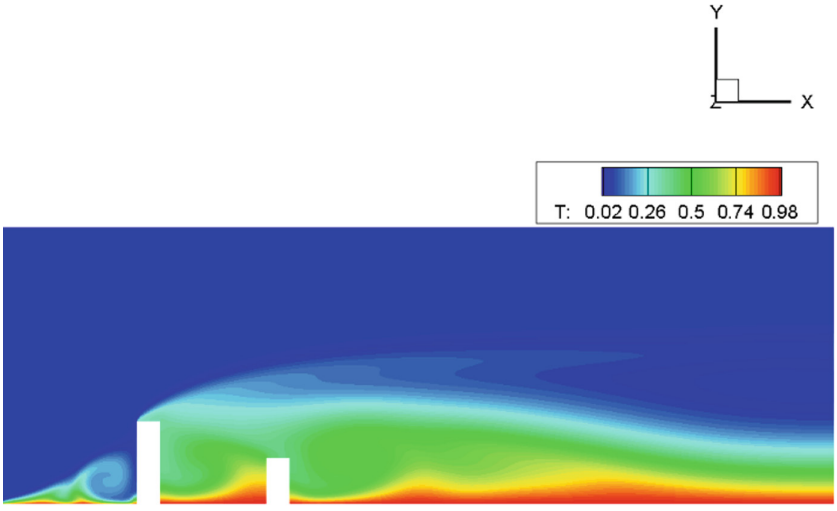

Fig. 13. Temperature component with buoyancy force for Pr = 0.7 and and $\Delta T = 1\,^{\circ}\mathrm{C}$.

Boundary conditions are specified for physical variables: pressure, temperature and velocity components: p pressure, u, v, w - velocity components, θ - temperature (Fig. 10).

In Fig. 11 shows horizontal velocity-component and streamlines with buoyancy force for Pr = 0.7 and $\Delta T = 1\,^{\circ}\mathrm{C}$. From Fig. 12 can be seen vertical velocity-component with buoyancy force for Pr = 0.7 and $\Delta T = 1\,^{\circ}\mathrm{C}$. In Fig. 13 can be seen temperature component with buoyancy force for Pr = 0.7 and

$\Delta T = 1\,^{\circ}\mathrm{C}$. The distance obtained for existing buildings was 35 m and satisfied all the standards specified in the republican standards. In the following case, the length of extensions to the buildings (balconies, porches, etc.) was added to the previous value and an approximate distance of 35 m was obtained. This model showed that a vortex in the gap occurs and therefore the natural purging between buildings is not broken.

7 Conclusion

Numerical studies of the laminar flow were carried out by the zone of joining the flows behind the backward-facing step with taking into account the buoyancy forces. This gave a deeper insight into the internal flow behind the backward-facing step and the processes of flows reconnection under the influence of temperature effects, which in turn gave an idea of the further appearance of secondary zones. The distance from the ledge to the canal boundary is 4 times the channel height, for a more detailed study of the backward-facing step flows with taking into account the buoyancy forces [9]. The numerical data of the velocity distribution showed the formation of a primary reattachment zone of backward-facing step flows. To numerically solve the Navier-Stokes equations system, the projection method was used. From numerical results can be seen that the realized numerical method gives a small error in comparison with the numerical results of other authors [9] for the dimensionless numbers $\mathrm{Re} = 50$, $\mathrm{Pr} = 0.7$ and $\mathrm{Gr} = 19.1$. After testing the numerical algorithm with the buoyancy forces, for the real problem considered a man-made obstacle with 9 floors (27 m) and 5 floors (15 m). In this problem, the wind speed was regarded as calm, according to the Beaufort wind speed scale (from 0 to 0.2 m/s). According to the data obtained as a result of the numerical simulation taking into account the buoyancy forces, it can be said that the current standards and rules for construction do not guarantee the required aerodynamics of the terrain. Also in this paper is used a parallel algorithm to obtain fast numerical results. This parallel algorithm is based on one-dimensional, two-dimensional and three-dimensional domain decomposition method. The numerical results from the 3D cavity flow test problem, which used 1D, 2D and 3D domain decomposition method showed that 3D domain decomposition is not time-consuming compared to 2D domain decomposition, for the number of processors that does not exceed 250, and 3D domain decomposition has more time-consuming software implementation and the use of 2D domain decomposition is sufficient for the scope of the problem. That's why for backward-facing step flow with vertical buoyancy force is used 2D domain decomposition. It should also be noted that setting the boundary conditions is an important process. In the future, this mathematical model and a parallel numerical algorithm can be applied to various complex flows taking into account the buoyancy forces.

References

1. Abbott, D.E., Kline, S.J.: Experimental investigations of subsonic turbulent flow over single and double backward-facing steps. J. Basic Eng. **84**, 317 (1962)
2. Sebanr, A.: Heat transfer to the turbulent separated flows of air downstream of a step in the surface of a plate. J. Heat Transf. **86**, 259 (1964)
3. Goldsteinr, J., Eriksenv, L., Olsonr, M., Eckerte, R.G.: Laminar separation, reattachment and transition of flow over a downstream-facing step. J. Basic Eng. **92**, 732 (1970)
4. Durst, F., Whitelawj, H.: Aerodynamic properties of separated gas flows: existing measurements techniques and new optical geometry for the laser-Doppler anemometer. Prog. Heat Mass Transf. **4**, 311 (1971)
5. Gosmana, D., Punw, M.: Lecture notes for course entitled: calculation of recirculating flow. Heat Transf. Rep. **74**, 2 (1974)
6. Kumara, Y.S.: Internal separated flows at large Reynolds number. J. Fluid Mech. **97**, 27 (1980)
7. Chiang, T.P., Tony, W.H., Sheu, Fang C.C.: Numerical investigation of vortical evolution in backward-facing step expansion flow. Appl. Math. **23**, 915–932 (1999)
8. Fletcher, C.A.J.: Computational Techniques for Fluid Dynamics, vol. 1, p. 387. Springer, New York (1988). https://doi.org/10.1007/978-3-642-58229-5
9. Lin, J.T., Armaly, B.F., Chen, T.S.: Mixed convection in buoyancy-assisting, vertical backward-facing step flows. Int. J. Heat Mass Transf. **33**(10), 2121–2132 (1990)
10. Armaly, B.F., Durst, F.: Reattachment length and recirculation regions downstream of two dimensional single backward facing step. In: Momentum and Hear Transfer Process in Recirculating Flows, ASME HTD, vol. 13, pp. 1–7. ASME, New York (1980)
11. Eaton, J.K., Johnson, J.P.: A review of research on subsonic turbulent flow reattachment. AIAA J. **19**, 1093–1100 (1981)
12. Simpson, R.L.: A review of some phenomena in turbulent flow separation. J. Fluid Eng. **103**, 520–530 (1981)
13. Aung, W.: An experimental study of laminar heat transfer downstream of backsteps. J. Heat Transf. **105**, 823–829 (1983)
14. Aung, W.: Separated forced convection. In: Proceedings of ASMEIJSME Thermal Enana Joint Conference, vol. 2, pp. 499–515. ASME, New York (1983)
15. Aung, W., Baron, A., Tsou, F.K.: Wall independency and effect of initial shear-layer thickness in separated flow and heat transfer. Int. J. Hear Muss Transf. **28**, 1757–1771 (1985)
16. Aung, W., Worku, G.: Theory of fully developed, combined convection including flow reversal. J. Hear Transf. **108**, 485–488 (1986)
17. Sparrow, E.M., Chrysler, G.M., Azevedo, L.F.: Observed flow reversals and measured-predicted Nusselt numbers for natural convection in a one-sided heated vertical channel. J. Heat Transf. **106**, 325–332 (1984)
18. Sparrow, E.M., Kang, S.S., Chuck, W.: Relation between the points of flow reattachment and maximum heat transfer for regions of flow separation. Int. J. Hear Mass Transf. **30**, 1237–1246 (1987)
19. Sparrow, E.M., Chuck, W.: PC solutions for heat transfer and fluid flow downstream of an abrupt, asymmetric enlargement in a channel. Numer. Hear Transf. **12**, 1940 (1987)
20. Chung, T.J.: Computational Fluid Dynamics (2002)

21. Issakhov, A.: Mathematical modeling of the discharged heat water effect on the aquatic environment from thermal power plant. Int. J. Nonlinear Sci. Numer. Simul. **16**(5), 229–238 (2015)
22. Issakhov, A.: Mathematical modeling of the discharged heat water effect on the aquatic environment from thermal power plant under various operational capacities. Appl. Math. Model. **40**(2), 1082–1096 (2016)
23. Issakhov, A.: Large eddy simulation of turbulent mixing by using 3D decomposition method. J. Phys.: Conf. Ser. **318**(4), 1282–1288 (2011)
24. Chorin, A.J.: Numerical solution of the Navier-Stokes equations. Math. Comp. **22**, 745–762 (1968)
25. Karniadakis, G.E., Kirby II, R.M.: Parallel Scientific Computing in C++ and MPI: A Seamless Approach to Parallel Algorithms and their Implementation. Cambridge University Press, Cambridge (2000)
26. Ngo, I., Byon, C.: Effects of heater location and heater size on the natural convection heat transfer in a square cavity using finite element method. J. Mech. Sci. Technol. **29**(7), 2995 (2015)
27. Oztop, H.F., Abu-Nada, E.: Numerical study of natural convection in partially heated rectangular enclosures filled with nanofluids. Int. J. Heat. Fluid Flow **29**(5), 1326–1336 (2008)
28. Xie, W.A., Xi, G.N.: Geometry effect on flow fluctuation and heat transfer in unsteady forced convection over backward and forward facing steps. Energy **132**, 49–56 (2017)
29. Yilmaz, I., Oztop, H.F.: Turbulence forced convection heat transfer over double forward facing step flow. Int. Commun. Heat Mass Transf. **33**, 508–517 (2006)
30. Xie, W.A., Xi, G.N., Zhong, M.B.: Effect of the vortical structure on heat transfer in the transitional flow over a backward-facing step. Int. J. Refrig. **74**, 463–472 (2017)
31. Issakhov, A.: Modeling of synthetic turbulence generation in boundary layer by using zonal RANS/LES method. Int. J. Nonlinear Sci. Numer. Simul. **15**(2), 115–120 (2014)
32. Issakhov, A.: Numerical modelling of distribution the discharged heat water from thermal power plant on the aquatic environment. In: AIP Conference Proceedings, vol. 1738, p. 480025 (2016)
33. Issakhov, A.: Numerical study of the discharged heat water effect on the aquatic environment from thermal power plant by using two water discharged pipes. Int. J. Nonlinear Sci. Numer. Simul. **18**(6), 469–483 (2017)
34. Issakhov, A.: Numerical modelling of the thermal effects on the aquatic environment from the thermal power plant by using two water discharge pipes. In: AIP Conference Proceedings, vol. 1863, p. 560050 (2017)
35. Issakhov, A., Zhandaulet, Y., Nogaeva, A.: Numerical simulation of dam break flow for various forms of the obstacle by VOF method. Int. J. Multiph. Flow **109**, 191–206 (2018)
36. Issakhov, A., Abylkassymova, A.: Application of parallel computing technologies for numerical simulation of air transport in the human nasal cavity. In: Zelinka, I., Vasant, P., Duy, V.H., Dao, T.T. (eds.) Innovative Computing, Optimization and Its Applications. SCI, vol. 741, pp. 131–149. Springer, Cham (2018). https://doi.org/10.1007/978-3-319-66984-7_8

37. Issakhov, A., Mashenkova, A.: Numerical study for the assessment of pollutant dispersion from a thermal power plant under the different temperature regimes. Int. J. Environ. Sci. Technol. 1–24 (2019). https://doi.org/10.1007/s13762-019-02211-y
38. Issakhov, A., Bulgakov, R., Zhandaulet, Y.: Numerical simulation of the dynamics of particle motion with different sizes. Eng. Appl. Comput. Fluid Mech. **13**(1), 1–25 (2019)